Nonlinear Dyn (2020) 100:2699–2714
https://doi.org/10.1007/s11071-020-05668-6

ORIGINAL PAPER

Complete dynamical analysis of a neocortical network model

Ali Foroutannia · Mahdieh Ghasemi · Fatemeh Parastesh · Sajad Jafari · Matjaž Perc

Received: 31 January 2020 / Accepted: 27 April 2020 / Published online: 14 May 2020

Abstract The brain is a complex system consisting of a large number of interacting neurons. Recently, a simple nonlinear biological model has been proposed for the up and down state transitions in the network of excitatory and inhibitory neurons. In this paper, we study the dynamical behavior of this model by calculating the Lyapunov exponents and bifurcation diagrams for various values of synaptic connections. We show that varying the synaptic strength values has a considerable effect on the bifurcations in the model. Furthermore, we show that the model can exhibit chaotic firing for certain values of the excitatory–excitatory synaptic strength.

Keywords Biological neuron models · Chaos · Excitatory and inhibitory synapses · Bifurcation

A. Foroutannia · M. Ghasemi
Neural Engineering Laboratory, Department of Biomedical Engineering, University of Neyshabur, Neyshabur, Iran

F. Parastesh · S. Jafari
Department of Biomedical Engineering, Amirkabir University of Technology, 424 Hafez Ave., Tehran 15875-4413, Iran

S. Jafari
Health Technology Research Institute, Amirkabir University of Technology, 424 Hafez Ave., Tehran 15875-4413, Iran

M. Perc (✉)
Faculty of Natural Sciences and Mathematics, University of Maribor, Koroška cesta 160, 2000 Maribor, Slovenia
e-mail: matjaz.perc@gmail.com

M. Perc
Department of Medical Research, China Medical University Hospital, China Medical University, Taichung, Taiwan

M. Perc
Complexity Science Hub Vienna, Josefstädterstraße 39, 1080 Vienna, Austria

1 Introduction

The nerve cells, which are known as the neurons, communicate with each other through the synapses [1]. A neuron consists of a cell body (soma), dendrites, and a single axon. Neurons receive signals through the dendrites and the soma and send signals to the axons. In most synapses, the signals are transmitted from the axon of one neuron to the dendrites of the other one [2]. The neurons are divided into two groups: excitatory and inhibitory neurons. Excitatory postsynaptic potential (EPSP) creates action potential. This temporary depolarization of the postsynaptic membrane potential is due to the influx of positively charged ions into the postsynaptic cell, resulting from the opening of ligand-gated ion channels [3]. In contrast, inhibitory postsynaptic potentials (IPSPs) are caused by the flow of negative ions into the cell or positive ions out of the cell [4]. Figure 1 shows the relationship between excitatory and inhibitory neurons in a brain region.

Biological neural models aim to explain the underlying mechanisms of the nervous system function [5]. These models provide a mathematical explanation of

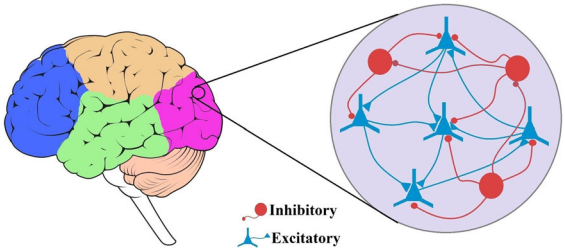

Fig. 1 Connections of the excitatory (blue) and inhibitory (red) neurons in the cerebral cortex. (Color figure online)

the characteristics of the nervous system that trigger the electrical potentials of the neuronal membranes [6,7]. The important aspects in biological models are the validation of experiments, and survey of the parameters variations on the system stability, and the use of physical units to describe the parameters. Neuron models can be divided into two categories according to the physical units of the model interface [8]: (1) the input–output membrane voltage models, such as the leaky integrate and fire model [9], Hodgkin–Huxley model [10], etc., and (2) the chemical input neuron models, such as synaptic transmission model [9] and the two-state Markov model [11]. Since the models of the first type are more popular, some of them [9,10,12–16] are summarized in Table 1. By increasing the experimental knowledge about the neurons, modified neuronal models were presented to indicate the effects of

Table 1 Some of the well-known biological neural models

Neuron model	Equations	Description	References
Leaky integrate and fire model	$I(t) - \frac{V_m(t)}{R_m} = C_m \frac{dV_m(t)}{dt}$ $f(I) = \begin{cases} 0, & I \le I_{th} \\ [t_{ref} - R_m C_m \log(1 - \frac{V_{th}}{I R_m})]^{-1}, & I > I_{th} \end{cases}$	I: Current that enters the neuron; $V(t)$: membrane potential; R_m: membrane resistance; C_m: lipid bilayer as a capacitance; I_{th}: current threshold; $f(I)$: firing frequency	[9]
FitzHugh–Nagumo model (FHN)	$\dot{v} = v - \frac{v^3}{3} - \omega + I_{ext}$ $\tau\dot{\omega} = v + a - b\omega$	v: Nonlinear elevation of the membrane voltage; ω: linear recovery variable; I_{ext}: applied current; τ: time constant; a, b: control parameters	[12,13]
Hindmarsh–Rose model	$\frac{dx}{dt} = y - ax^3 + bx^2 - z + I$ $\frac{dy}{dt} = c - dx^2 - y$ $\frac{dz}{dt} = r(e(x + f) - z)$ $r^2 = x^2 + y^2 + z^2$	$x(t)$: Membrane potential; $y(t), z(t)$: transport of ions across the membrane through the ion channels; I: current that enters the neuron; a, b, c, d, r, e, f: control parameters	[14]
Hodgkin–Huxley model	$C_m \frac{dV(t)}{dt} = -\sum_i I_i(t, V)$ $I(t, V) = g(t, V)(V - V_{eq})$ $g(t, V) = \bar{g} m(t, V)^p h(t, V)^q$ $\frac{dm(t,V)}{dt} = \frac{m_\infty(V) - m(t,V)}{\tau_m(V)} = \alpha_m(V)(1 - m) - \beta_m(V)m$	$V(t)$: Membrane potential; C_m: lipid bilayer as a capacitance; $I(t, V)$: current that enters the neuron; $g(t, V)$: conductance; $m(t, V), h(t, V)$: number of ions passing through the membrane channels; $\tau_m(V), \alpha_m(V), \beta_m(V)$: gate fractions	[10]
Morris–Lecar model	$C\frac{dV}{dt} = -I_{ion}(V, \omega) + I$ $\frac{d\omega}{dt} = \varphi \frac{\omega_\infty - \omega}{\tau_\omega}$ $I_{ion}(V, \omega) = \bar{g}_{ca} m_\infty (V - V_{ca}) + \bar{g}_K \omega (V - V_K) + \bar{g}_L (V - V_L)$	V: Membrane potential; ω: recovery variable the probability that the K^+ channel is conducting; I: applied current; C: membrane capacitance; $\bar{g}_{ca}$ $\bar{g}_K$, $\bar{g}_L$: leak, Ca^{++}, and K^+ conductance's through membranes channel; V_L, V_{ca}, V_K: equilibrium potential of relevant ion channels; φ: reference frequency	[15]
Exponential integrate and fire model	$\frac{dV}{dt} = \frac{1}{\tau_m}[E_m - V + \Delta_T \exp(\frac{V - V_T}{\Delta_T})]$	V: Membrane potential; Δ_T: membrane potential threshold; τ_m: membrane time constant; E_m: resting potential; V_T: sharpness of action potential initiation	[16]

different factors on the neuronal behaviors. For example, in some researches, the effect of the electromagnetic induction on the behavior of the neuron has been considered [17–21]. In 2016, Lv and Ma [22] introduced a new neuron model capable of describing the effects of the electromagnetic field. Very recently, Wu et al. [23] used charge-controlled and flux-controlled memristors in a neuron model for characterizing the time-varying electromagnetic field, which is the result of the continuous ionic flux. Xu et al. [24] modified the Hodgkin–Huxley model by considering the effect of the temperature on the neuron's membrane voltage. They also applied the memristor for the ion channels and investigated different behaviors of the new model by applying an external stimulus. In addition to the complex dynamics of the neuron models, the collective behaviors of the network of coupled neural models have been investigated extensively [25–29].

Analyzing the dynamics of the neural models is of great importance. Some of the previous studies were devoted to the investigation of the dynamics of the neuron models, specifically chaotic firings. For example, Vaidyanathan [30] examined the qualitative features of the chaotic FitzHugh–Nagumo (FHN) neuron model and also found the results for its output regulation via the adaptive control method. Lakshmanan et al. [31] analyzed the chaotic firing of the HR neuron with state-dependent time delays via time series, bifurcation diagram, and Lyapunov exponents. Panahi et al. [32] extracted the dynamical properties of the magnetic neuron model and also presented an implementation of the electronic circuit. The robustness of the neural models against noise has also been studied [33–35].

In 2012, Ghorbani et al. [7] developed a simple nonlinear dynamic model for the up and down state neuronal cortex oscillations based on dendritic spike frequency adaptation. In fact, they presented a three-dimensional model for a set of coupled inhibitory and excitatory neurons and called it uniform network model. It is notable that this model is different from general neuronal networks which are obtained by coupling a number of neuron's models. Their model is consistent with the following features: (i) In the limit cycle mode, the neocortical neurons rarely fire at a rate of 1 Hz, (ii) in the down state of oscillatory activity, the membrane potential of different types of neurons is hyperpolarized, (iii) the up-state activity is regulated by inhibitory neurons, (iv) up- and down-state oscillations are synchronized across the large sections of the cortex. The up–down state (UDS) oscillations refer to the cycle between up and down state potentials [36]. This is used to examine the relationship between connectivity and the dynamics of cerebral and neural circuits. These oscillations can be explained by the variability of neural responses to stimuli. The researches have shown that during UDS the neocortex and the hippocampus develop long-term memory [37–40]. Slow wave sleep (SWS), often referred as deep sleep, is related to the UDS oscillations and comprises the third and fourth stages of the four sleep stages. Subsequent studies showed that during UDS in the sleep, the excitatory and inhibitory neurons change simultaneously. Therefore, UDS can be described by the firing rate of a set of neurons [41–43]. It has been shown that in these neuronal behaviors, the range of biological parameters can be extracted from the chaotic parts [44,45]. Some studies have revealed that the chaotic dynamics occur in sleep [46]. In [47], the chaotic behavior of neurons was examined by computing the entropy and it was shown that the entropy is greater during deep sleep. In another research [48], the level of chaos in the deep sleep of mice and its relation with the age were studied, and it was found that the chaos level increases with age. Overall, these fluctuations in the brain can lead to motivational forgetfulness, memory stabilization, and brain activity increment [49,50]. In this study, we consider the model presented in [7] and investigate the dynamical properties of these equations. The bifurcation diagrams and the Lyapunov exponents of the model are presented and different periodic, and chaotic behaviors are demonstrated.

2 Model description

The binding of one excitatory neuron and one inhibitory neuron is shown in Fig. 2. The strengths of the synapses are denoted by J, such that $J_{ee} > 0$ is the synaptic strength of the excitatory neuron to excitatory neuron, $J_{ei} > 0$ is the synaptic strength of the excitatory neuron to inhibitory neuron, $J_{ie} < 0$ is the synaptic strength of the inhibitory neuron to excitatory neuron, and $J_{ii} < 0$ is the synaptic strength of the inhibitory neuron to inhibitory neuron. These 4 parameters determine the firing rate of the neurons.

The model presented by Ghorbani et al. [7] considers that the coupled excitatory and inhibitory neurons are

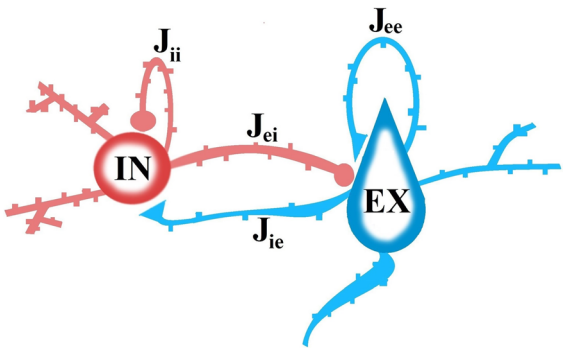

Fig. 2 Two coupled excitatory and inhibitory neurons. The relationship between excitatory and inhibitory neurons is bidirectional

evoked by the potential of the neurons' membranes and the adaptation parameter. The equations describing the firing of the excitatory and inhibitory neurons are as follows:

$$\frac{dv_e}{dt} = -\frac{1}{\tau_e}v_e + N_e J_{ee}(c) r(v_e) + N_i J_{ei} r(v_i)$$

$$\frac{dv_i}{dt} = -\frac{1}{\tau_i}v_i + N_i J_{ii} r(v_i) + N_e J_{ie} r(v_e)$$

$$\frac{dc}{dt} = -\frac{1}{\tau_c}c + N_e \Delta c r(v_e) \quad (1)$$

where v_e ,v_i are the membrane potential of excitatory and inhibitory neurons, and c is the adaptability parameter which is used in a description similar to Fuhrman et al. [51]. τ_e and τ_i represent the time constants of relaxation of the excitatory and inhibitory neuron membrane potential, and τ_c denotes the time of recovery of adaptation between neurons, assuming that the resting potential is constant for all different neuron types. The N_e and N_i represent the number of excitatory and inhibitory neurons in the network. The authors in Ref. [7] have assumed that the maximum number of connected neurons is $N = 10{,}000$, from which $0.2 \times 10{,}000$ are the inhibitory neurons and $0.8 \times 10{,}000$ are the excitatory neurons. Finally, the number of neurons is multiplied by 0.2 to indicate the likelihood of neurons connecting. $J_{ee}(c)$ is dependent on the adaptation parameter such that if the adaptation parameter c exceeds a threshold, the synaptic strength decreases rapidly, defined by the

Table 2 The model parameters are defined within the table

Parameter	Unit	Value	Define
τ_e	s	0.02	Temporal constant of excitatory neuron membrane
τ_i	s	0.01	Temporal constant of inhibitory neuron membrane
τ_c	s	0.5	Time constant recovery adaptive
N_e	–	$(0.8 \times 10{,}000) \times 0.2$	The number of excitatory neurons in the network
N_i	–	$(0.2 \times 10{,}000) \times 0.2$	The number of inhibitory neurons in the network
$J_{ee}(0)$	mV	0.74	Synaptic strength of the excitatory neuron to excitatory neuron
J_{ei}	mV	1.75	Synaptic strength of the excitatory neurons to inhibitory neurons
J_{ii}	mV	0.35	Synaptic strength of the inhibitory neuron to inhibitory neuron
J_{ie}	mV	0.8	Synaptic strength of inhibitory neurons to excitatory neurons
Δc	mV	0.015	Average adaptive parameter
c^*	mV	10	Average adaptive threshold
v^*	mV	30	Potential of excitation threshold
g_c	mV	3	Inverse slope of average compatibility
g_i	mV	2	Inverse gradient dependence of inhibitory neuron excitation rate on membrane potential
g_e	mV	5	Inverse gradient dependence of excitatory neuron excitation rate on membrane potential
r_m	Hz	70	Maximum excitement cadence

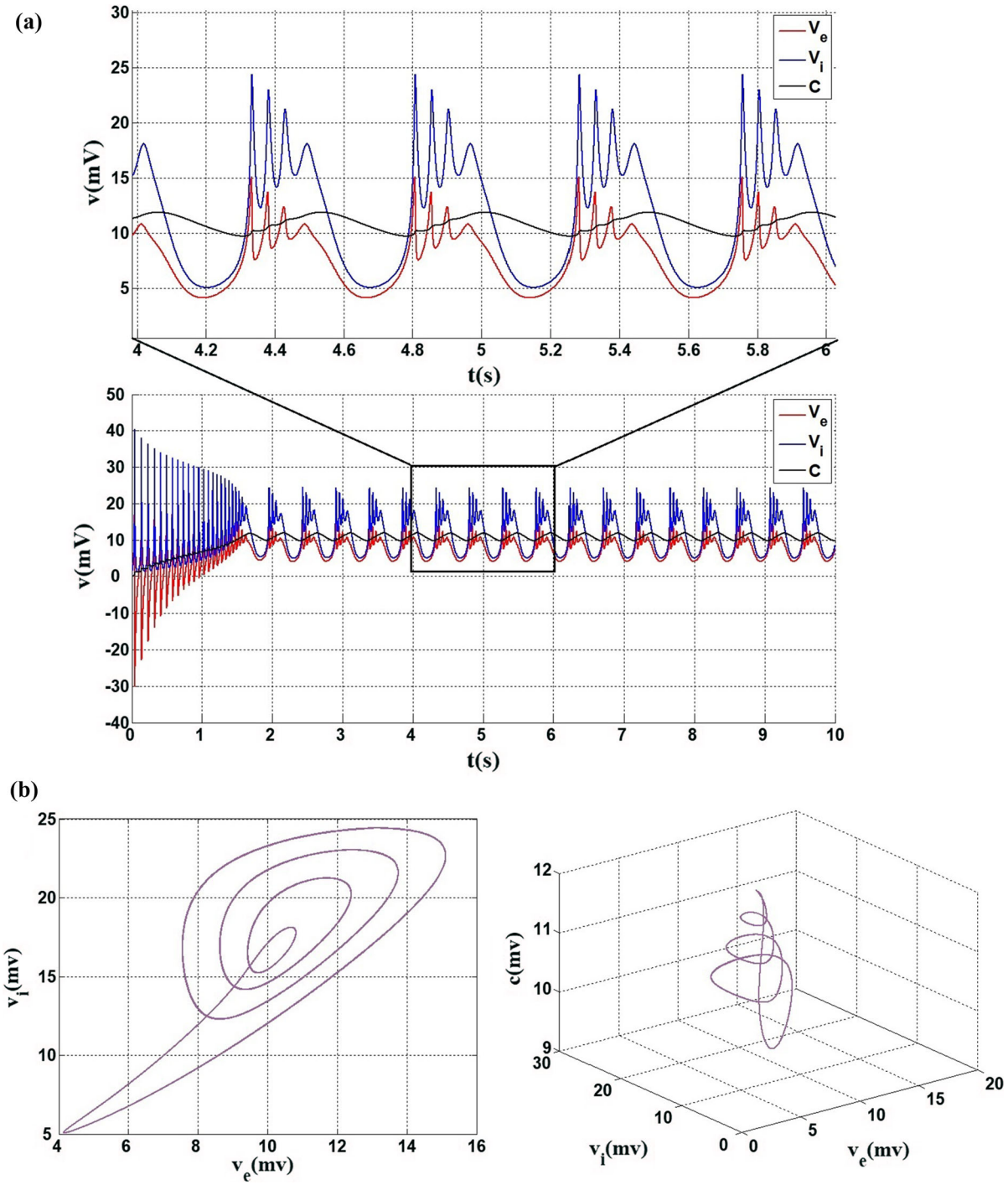

Fig. 3 **a** The time series of the model of Eq. 1 by setting the parameters at the values given in Table 2. **b** The corresponding attractor of the model. By setting these values the model exhibits a periodic behavior

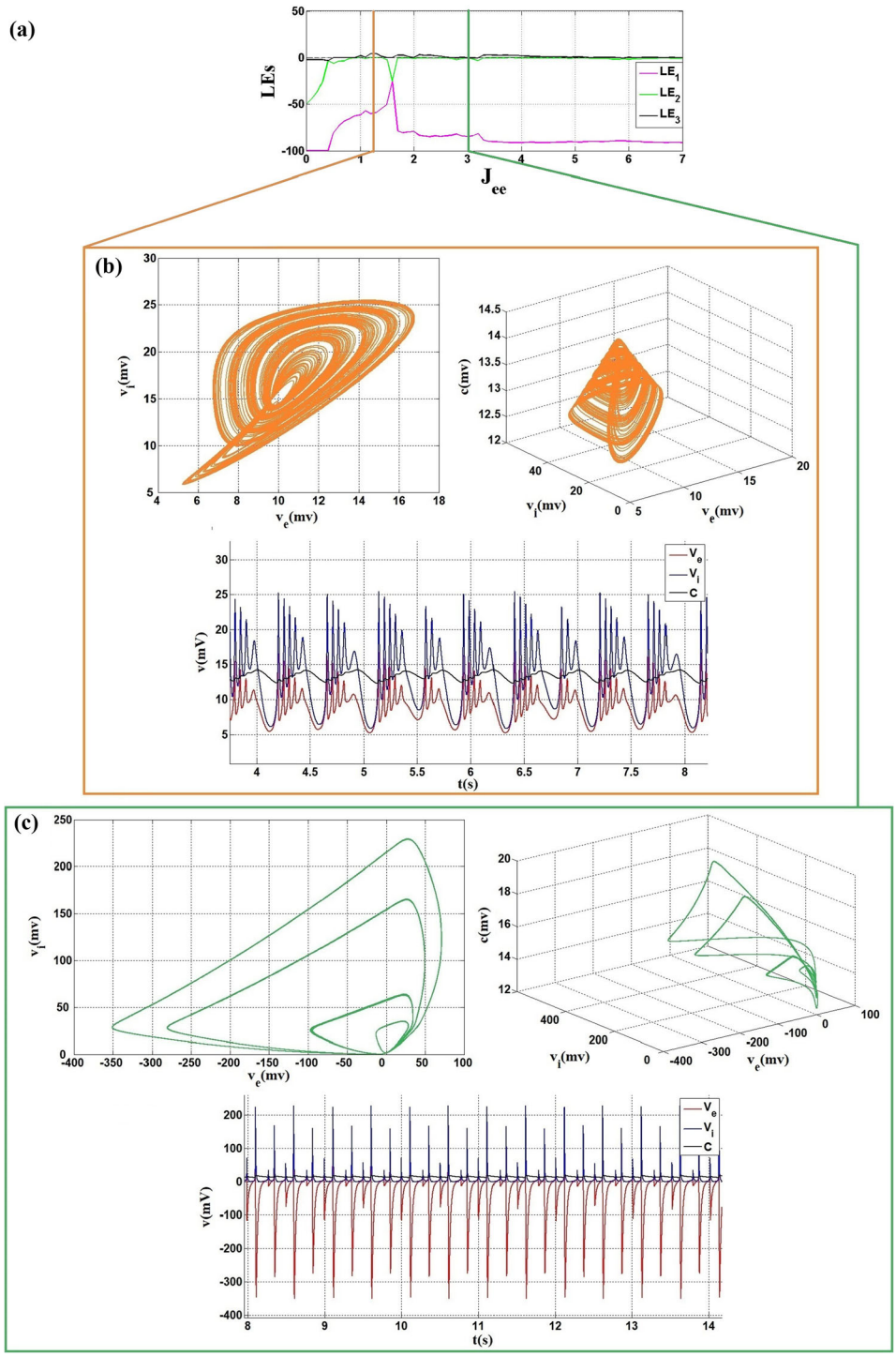

Fig. 4 **a** The Lyapunov exponents of the model with respect to J_{ee}, in the interval [0, 5]. By changing the value of J_{ee}, the model is capable of showing different dynamical behavior. **b** The attractor and the time series of the model for $J_{ee} = 1.25$, at which the model exhibits chaotic behavior. **c** The attractor and the time series of the model for $J_{ee} = 2.95$, at which the behavior is periodic

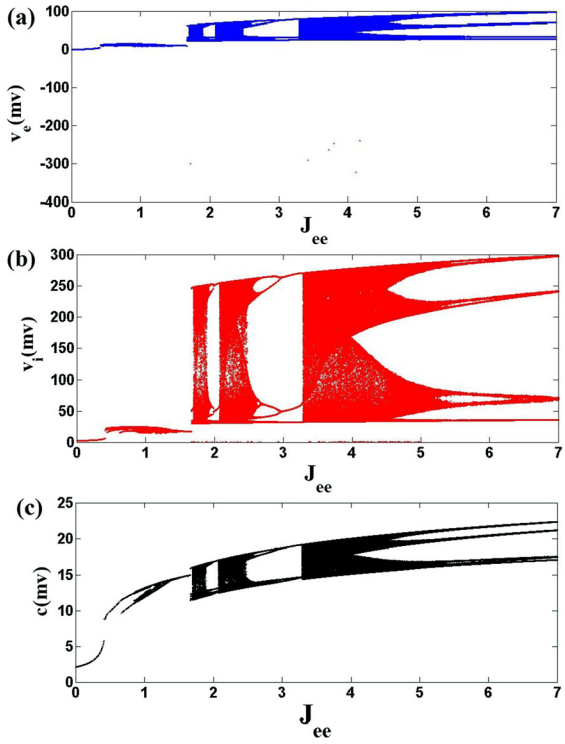

Fig. 5 The bifurcation diagrams (local maximum of the time series) with respect to J_{ee} in the interval [0, 5]. The model shows chaotic behavior in a wide region of J_{ee}. **a** Excitatory membrane potential v_e, **b** inhibitory membrane potential v_i, and **c** adaptive parameter c

following sigmoidal relation:

$$J_{ee}(c) = \frac{J_{ee}(0)}{1 + \exp\left[\frac{c-c^*}{g_c}\right]} \tag{2}$$

The parameter g_c is the inverse of the adaptation slope, and c^* indicates the adaptation threshold. The dependence of the firing rate of a neuron on the membrane potential is defined by:

$$r(v_{e,i}) = \frac{r_m}{1 + \exp\left[-\frac{v_{e,i}-v^*}{g_{c,i}}\right]} \tag{3}$$

Here, $r_m(\sim 70\,\text{Hz})$ is the maximum firing rate at full depolarization, and v^* is the threshold of firing potential. $g_{e,i}$ is the dependence of the firing rate on the membrane potential for excitatory/inhibitory neuron. The parameters used in this paper are presented in Table 2. The time series and the attractor of the uniform network are plotted in Fig. 3.

3 Dynamical analysis

In this section, the dynamical behavior of the model of Eqs. 1–3 is analyzed by extracting Lyapunov exponents and bifurcation diagrams. The Lyapunov exponents of a system determine the degree of separation of infinitely close trajectories [52]. These values are calculated by the following equation:

$$\dot{Y} = JY \tag{4}$$

where matrix Y explains that small changes in initial conditions are propagated to the end point. The matrix J is the Jacobian matrix of the model Eq. 1, calculated at [0, 0, 0] as follows:

$$J = \frac{\mathrm{d}f_i(x)}{\mathrm{d}x_i}|_{x(t)} = \begin{bmatrix} a_{11} & a_{12} & a_{13} \\ a_{21} & a_{22} & a_{23} \\ a_{31} & a_{32} & a_{33} \end{bmatrix} \tag{5}$$

With

$$a_{11} = \frac{N_e J_{ee} r_m \exp\left[-\frac{v_e-v^*}{g_e}\right]}{g_e\left(\exp\left[\frac{c-c^*}{g_e}\right]+1\right)\left(\exp\left[-\frac{v_e-v^*}{g_e}\right]+1\right)^2} - \frac{1}{\tau_e}$$

$$a_{12} = -\frac{N_i J_{ei} r_m \exp\left[-\frac{v_i-v^*}{g_i}\right]}{g_i\left(\exp\left[-\frac{v_i-v^*}{g_i}\right]+1\right)^2}$$

$$a_{13} = \frac{N_e J_{ee} r_m \exp\left[\frac{c-c^*}{g_c}\right]}{g_c\left(\exp\left[\frac{c-c^*}{g_c}\right]+1\right)^2\left(\exp\left[-\frac{v_e-v^*}{g_e}\right]+1\right)}$$

$$a_{21} = \frac{N_e J_{ie} r_m \exp\left[-\frac{v_e-v^*}{g_e}\right]}{g_e\left(\exp\left[-\frac{v_e-v^*}{g_e}\right]+1\right)^2}$$

$$a_{22} = -\frac{1}{\tau_i} - \frac{N_i J_{ii} r_m \exp\left[-\frac{v_i-v^*}{g_i}\right]}{g_i\left(\exp\left[-\frac{v_i-v^*}{g_i}\right]+1\right)^2}$$

$$a_{23} = 0$$

$$a_{31} = \frac{N_e \Delta c r_m \exp\left[-\frac{v_e-v^*}{g_e}\right]}{g_e\left(\exp\left[-\frac{v_e-v^*}{g_e}\right]+1\right)^2}$$

$$a_{32} = 0$$

Table 3 The transitions between different dynamics of the model by J_{ee} variation in the range of [0, 5] (LE_1, LE_2, and LE_3 denote the three Lyapunov exponents)

Parameter range	Lyapunov exponents value	Dynamical behavior		
		v_e	v_i	c
$0 \leq J_{ee} < 0.43$	At $J_{ee} = 0.215$	Fixed point	Fixed point	Fixed point
	$LE_1 = -99.96, LE_2 = -35.40, LE_3 = -2.07$			
$0.43 \leq J_{ee} < 0.63$	At $J_{ee} = 0.530$	Period 3	Period 3	Period 1
	$LE_1 = -78.19, LE_2 = -5.82, LE_3 \approx 0$			
$0.63 \leq J_{ee} < 0.9$	At $J_{ee} = 0.740$	Period 4	Period 4	Period 2
	$LE_1 = -67.40, LE_2 = -2.10, LE_3 \approx 0$			
$0.9 \leq J_{ee} < 1.1$	At $J_{ee} = 1.000$	Chaos	Chaos	Chaos
	$LE_1 = -61.68, LE_2 \approx 0, LE_3 = 2.04$			
$1.1 \leq J_{ee} < 1.14$	At $J_{ee} = 1.120$	Period 8	Period 8	Period 6
	$LE_1 = -54.84, LE_2 = -2.09, LE_3 \approx 0$			
$1.14 \leq J_{ee} < 1.36$	At $J_{ee} = 1.250$	Chaos	Chaos	Chaos
	$LE_1 = -55.95, LE_2 \approx 0, LE_3 = 1.30$			
$1.36 \leq J_{ee} < 1.68$	At $J_{ee} = 1.520$	Period 1	Period 1	Period 1
	$LE_1 = -51.15, LE_2 = -0.91, LE_3 \approx 0$			
$1.68 \leq J_{ee} < 1.94$	At $J_{ee} = 1.810$	Chaos	Chaos	Chaos
	$LE_1 = -80.60, LE_2 \approx 0, LE_3 = 2.63$			
$1.94 \leq J_{ee} < 2.07$	At $J_{ee} = 2.005$	Period 4	Period 4	Period 4
	$LE_1 = -79.64, LE_2 = -0.21, LE_3 \approx 0$			
$2.07 \leq J_{ee} < 2.58$	At $J_{ee} = 2.325$	Chaos	Chaos	Chaos
	$LE_1 = -84.69, LE_2 \approx 0, LE_3 = 2.09$			
$2.58 \leq J_{ee} < 3.28$	At $J_{ee} = 2.930$	Period 5	Period 5	Period 6
	$LE_1 = -84.69, LE_2 = -0.39, LE_3 \approx 0$			
$3.28 \leq J_{ee} < 5$	At $J_{ee} = 4.140$	Chaos	Chaos	Chaos
	$LE_1 = -91.04, LE_2 \approx 0, LE_3 = 1.31$			

$$a_{33} = -\frac{1}{\tau_c}$$

Bifurcation analysis is the study of the qualitative changes of a system [53]. Here, we present the bifurcation analysis by plotting the local-maximum values of the time series of the model in five cases, according to the variations of the synaptic strength between excitatory and inhibitory neurons (J_{ee}, J_{ei}, J_{ie}, J_{ii}), and the adaptation parameter (Δc).

4 Result

The importance of interactions between neurons, which depends on the strength of the synapse, is undeniable. We show that the proposed neuronal model is capable of exhibiting chaotic behavior by changing the synaptic strengths. The Lyapunov exponents of the model by changing the excitatory–excitatory synaptic strength (J_{ee}) are demonstrated in Fig. 4. According to this figure, by increasing this synaptic strength, the largest Lyapunov exponent becomes positive at some J_{ee} values. The bifurcation diagrams of the model with respect to J_{ee} are represented in Fig. 5. As this figure shows, the model's behavior changes to chaotic behavior in a wide region. Furthermore, there are some periodic windows within the chaotic region. Figure 4b shows an example of the chaotic behavior of the model at $J_{ee} = 1.25$, and Fig. 4c illustrates a periodic firing for $J_{ee} = 2.95$. Table 3 presents the transitions between different dynamics of the model for $J_{ee} \in [0, 5]$ in detail.

Figures 6 and 7 illustrate the Lyapunov spectrum and the bifurcation diagrams of the model with respect to

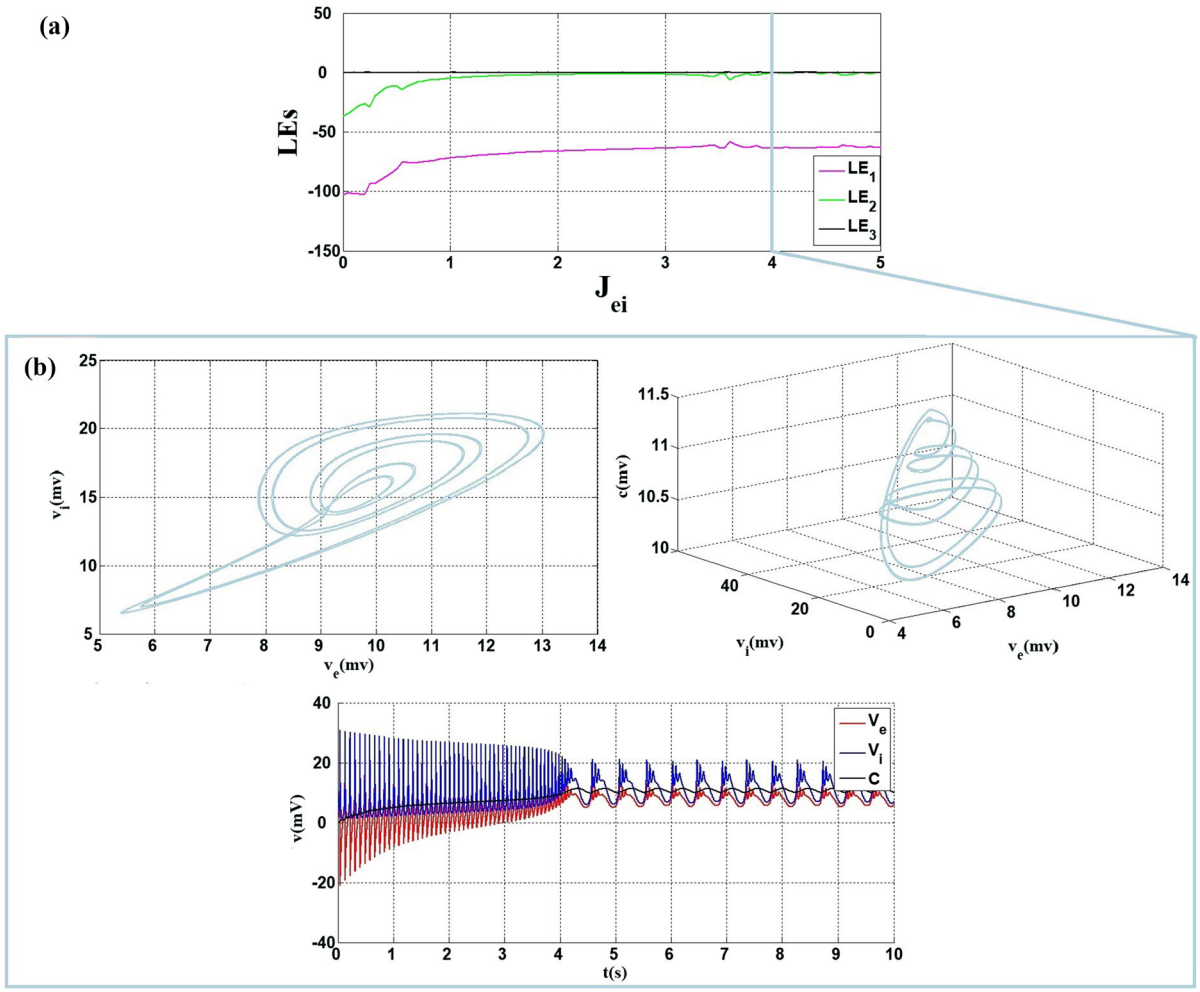

Fig. 6 **a** The Lyapunov exponents of the model with respect to J_{ei}, in the interval [0, 5]. The Lyapunov exponents are all negative by varying the value of J_{ei}. **b** The attractor and time series of the model for $J_{ei} = 4$, exhibiting a periodic behavior

the excitatory–inhibitory synaptic strength in the interval [0, 5]. According to the Lyapunov spectrum shown in Fig. 6a, the Lyapunov exponents are negative for all J_{ei} values, and thus, the model can only exhibit periodic behavior. Figure 6b shows the periodic firing of the system for $J_{ei} = 4$. The bifurcation diagrams in Fig. 7 demonstrate that by increasing this synaptic strength, the period of the firing of the neuron's membrane potential is firstly increased from period-1 to period-4 and then is turned back to period-1. The transitions between different periodic firings, by varying $J_{ei} \in [0, 5]$, are presented in Table 4.

The Lyapunov exponents and bifurcation diagrams of the model with respect to inhibitory–inhibitory synaptic strength are shown in Fig. 8 and 9, respectively. Figure 8 depicts that by varying the inhibitory–inhibitory synaptic strength, the model is only capable of showing periodic behavior, and the chaotic firing is not obtained. The bifurcation diagram demonstrates that for very small J_{ii} values, the neuron has period-1 firing. By increasing J_{ii}, the neuron bifurcates to a period-4 oscillation. Further increasing J_{ii} leads to the decrement of the period of the firing. Finally, at $J_{ii} = 2.07$ the membrane potential returns to period-1

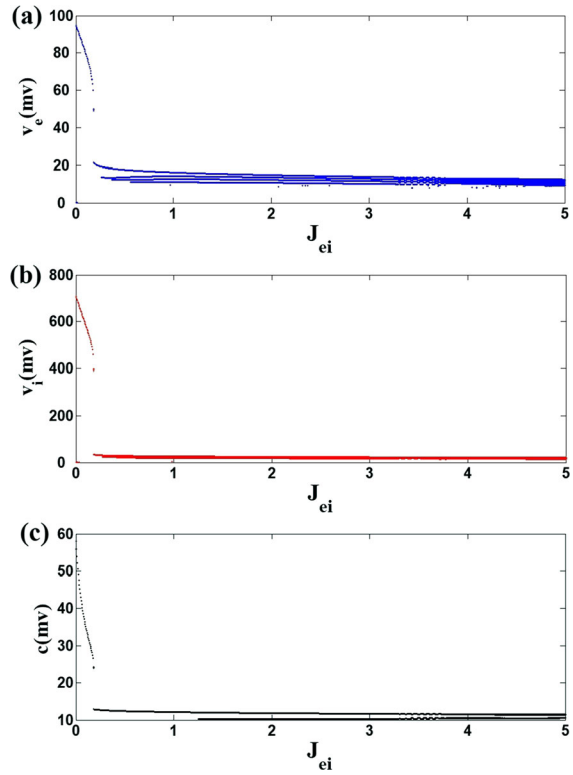

Fig. 7 The bifurcation diagrams (local maximum of the time series) with respect to J_{ei} in the interval [0, 5]. By increasing the J_{ei} value, the period of oscillations changes but the behavior is always periodic. **a** Excitatory membrane potential v_e, **b** inhibitory membrane potential v_i, and **c** adaptive parameter

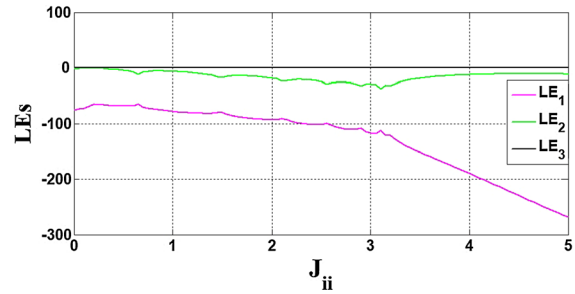

Fig. 8 The Lyapunov exponents of the model with respect to J_{ii}, in the interval [0, 5]. By varying the value of J_{ii}, all of the Lyapunov exponents are negative

oscillation. Table 5 shows the details of the behaviors of the neuron model by changing the inhibitory–inhibitory synaptic strength in the interval [0, 5].

The inhibitory–excitatory synaptic strength is the last synaptic strength, whose effect on the neuron's dynamics is investigated. Figure 10 shows the Lyapunov exponents of this case. This figure depicts that in the interval [0, 5], the model behaves only periodically. The bifurcation diagrams, which are shown in Fig. 11, illustrate that the membrane potential firing starts with period-1 oscillation, and then, the behavior is changed to period-4 firing and finally is attracted to an equilibrium at $J_{ie} = 1.1$. Table 6 presents different dynamics of the model for $J_{ie} \in [0, 5]$.

Table 4 The transitions between different dynamics of the model by J_{ei} variation in the range of [0, 5] (LE_1, LE_2, and LE_3 denote the three Lyapunov exponents)

Parameter range	Lyapunov exponents value	Dynamical behavior		
		v_e	v_i	c
$0 \leq J_{ei} < 0.27$	At $J_{ei} = 0.135$	Period 1	Period 1	Period 1
	$LE_1 = -100.93, LE_2 = -34.94, LE_3 \approx 0$			
$0.27 \leq J_{ei} < 0.39$	At $J_{ei} = 0.330$	Period 2	Period 2	Period 1
	$LE_1 = -10.41, LE_2 = -29.06, LE_3 \approx 0$			
$0.39 \leq J_{ei} < 0.615$	At $J_{ei} = 0.502$	Period 3	Period 3	Period 1
	$LE_1 = -97.54, LE_2 = -27.18, LE_3 \approx 0$			
$0.615 \leq J_{ei} < 1.25$	At $J_{ei} = 0.932$	Period 4	Period 4	Period 1
	$LE_1 = -84.59, LE_2 = -13.99, LE_3 \approx 0$			
$1.25 \leq J_{ei} < 5$	At $J_{ei} = 3.125$	Period 4	Period 4	Period 2
	$LE_1 = -65.63, LE_2 = -2.73, LE_3 \approx 0$			

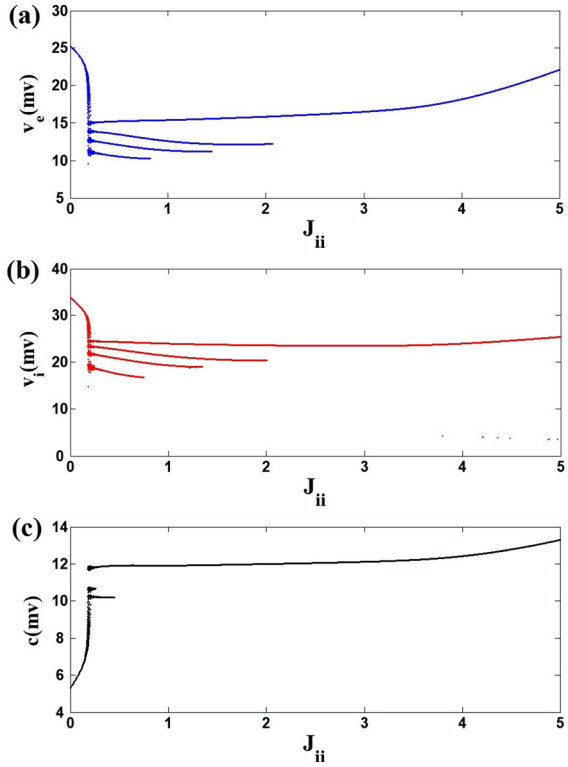

Fig. 9 The bifurcation diagrams (local maximum of the time series) with respect to J_{ii} in the interval [0, 5]. Similar to the J_{ei}, changing J_{ii} value does not lead to chaotic behavior. **a** Excitatory membrane potential v_{e}, **b** inhibitory membrane potential v_{i}, and **c** adaptive parameter

Finally, the effect of changing the adaptive parameter (Δc) on the dynamics of the neuronal model is investigated. Table 7 depicts different behaviors with varying this parameter. When $0 \leq \Delta c < 0.026$, the model has period-1 oscillation and for $\Delta c > 0.026$, reaches a rest state. Figure 12a shows the transition of the model from an initial state to the fixed point in the state space. The time series of the model variables in the rest state are illustrated in Fig. 12b.

Table 5 The transitions between different dynamics of the model by J_{ii} variation in the range of [0, 5] (LE_1, LE_2, and LE_3 denote the three Lyapunov exponents)

Parameter range	Lyapunov exponents value	Dynamical behavior		
		v_{e}	v_{i}	c
$0 \leq J_{\mathrm{ii}} < 0.12$	At $J_{\mathrm{ii}} = 0.060$	Period 1	Period 1	Period 1
	$\mathrm{LE}_1 = -75.22, \mathrm{LE}_2 = -2.24, \mathrm{LE}_3 \approx 0$			
$0.12 \leq J_{\mathrm{ii}} < 0.25$	At $J_{\mathrm{ii}} = 0.185$	Period 5	Period 5	Period 4
	$\mathrm{LE}_1 = -73, \mathrm{LE}_2 = -2, \mathrm{LE}_3 \approx 0$			
$0.25 \leq J_{\mathrm{ii}} < 0.44$	At $J_{\mathrm{ii}} = 0.345$	Period 4	Period 4	Period 2
	$\mathrm{LE}_1 = -68.12, \mathrm{LE}_2 = -1.52, \mathrm{LE}_3 \approx 0$			
$0.44 \leq J_{\mathrm{ii}} < 0.74$	At $J_{\mathrm{ii}} = 0.590$	Period 4	Period 4	Period 1
	$\mathrm{LE}_1 = -64.27, \mathrm{LE}_2 = -1.95, \mathrm{LE}_3 \approx 0$			
$0.74 \leq J_{\mathrm{ii}} < 0.82$	At $J_{\mathrm{ii}} = 0.780$	Period 4	Period 3	Period 1
	$\mathrm{LE}_1 = -64.73, \mathrm{LE}_2 = -3.11, \mathrm{LE}_3 \approx 0$			
$0.82 \leq J_{\mathrm{ii}} < 1.345$	At $J_{\mathrm{ii}} = 1.082$	Period 3	Period 3	Period 1
	$\mathrm{LE}_1 = -65.96, \mathrm{LE}_2 = -5.21, \mathrm{LE}_3 \approx 0$			
$1.345 \leq J_{\mathrm{ii}} < 1.445$	At $J_{\mathrm{ii}} = 1.400$	Period 3	Period 2	Period 1
	$\mathrm{LE}_1 = -67.36, \mathrm{LE}_2 = -7.76, \mathrm{LE}_3 \approx 0$			
$1.445 \leq J_{\mathrm{ii}} < 1.985$	At $J_{\mathrm{ii}} = 1.715$	Period 2	Period 2	Period 1
	$\mathrm{LE}_1 = -72.89, \mathrm{LE}_2 = -6.55, \mathrm{LE}_3 \approx 0$			
$1.985 \leq J_{\mathrm{ii}} < 2.07$	At $J_{\mathrm{ii}} = 2.027$	Period 2	Period 1	Period 1
	$\mathrm{LE}_1 = -77.21, \mathrm{LE}_2 = -7.67, \mathrm{LE}_3 \approx 0$			
$2.07 \leq J_{\mathrm{ii}} < 5$	At $J_{\mathrm{ii}} = 3.535$	Period 1	Period 1	Period 1
	$\mathrm{LE}_1 = -89.68, \mathrm{LE}_2 = -14.69, \mathrm{LE}_3 \approx 0$			

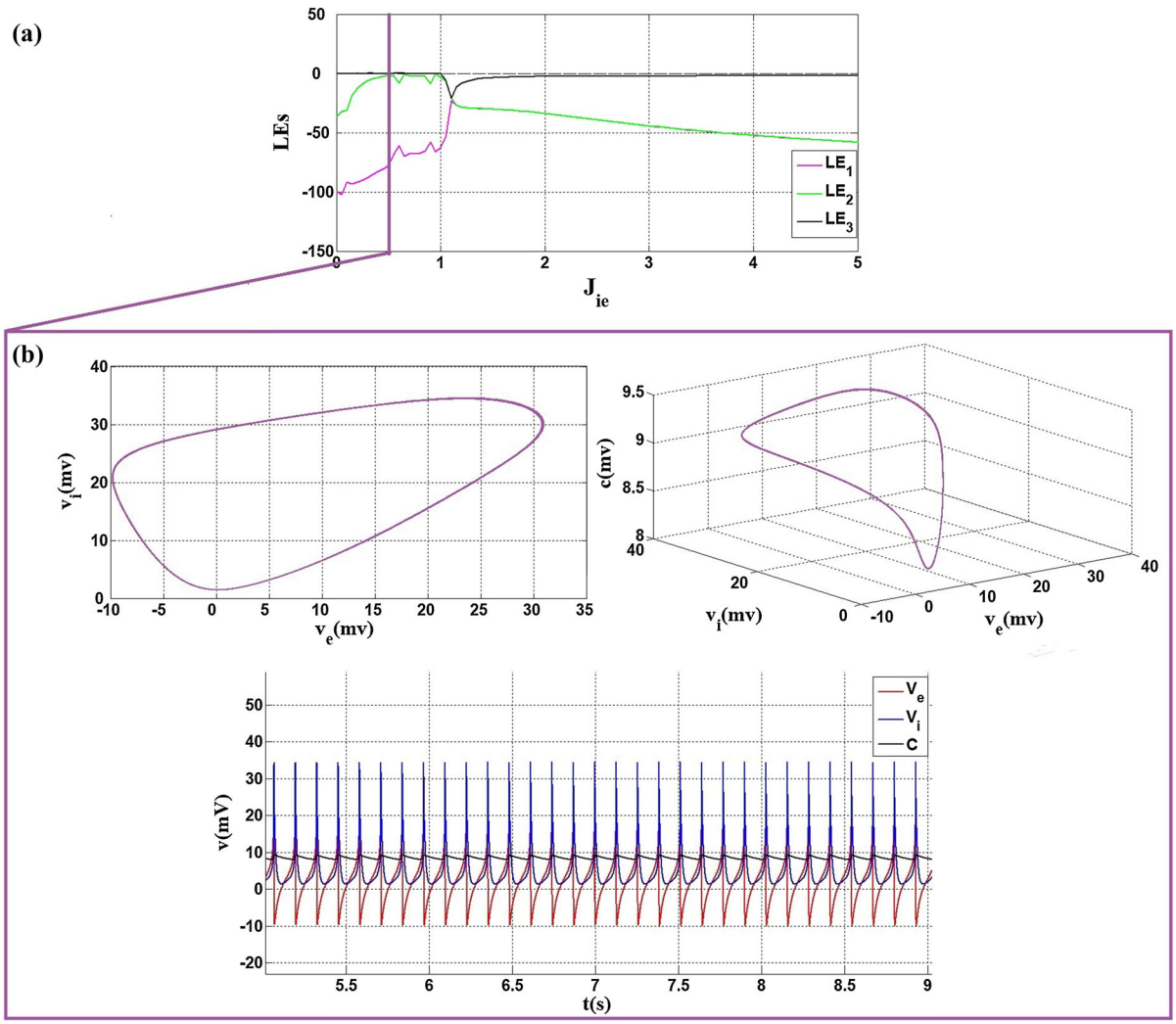

Fig. 10 **a** The Lyapunov exponents of the model with respect to J_{ie}, in the interval [0, 5]. The Lyapunov exponents are all negative. **b** The attractor and the time series of the model for $J_{\mathrm{ie}} = 0.5$, exhibiting a periodic behavior

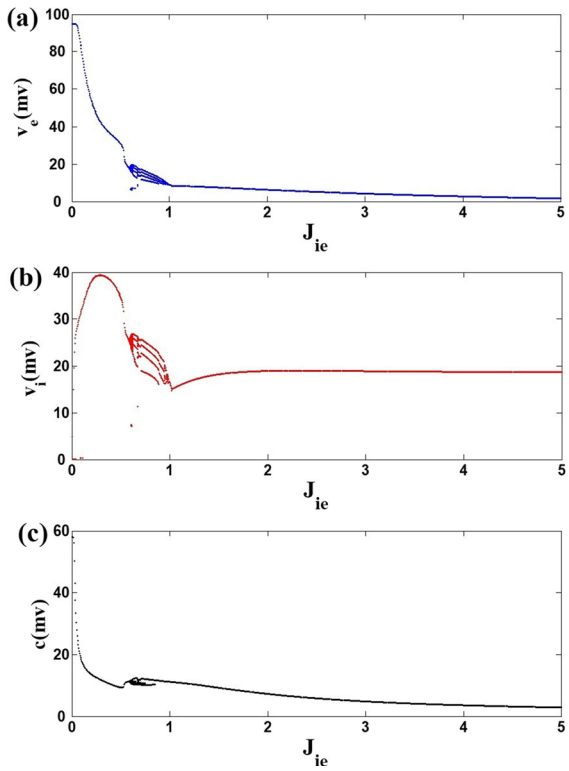

Fig. 11 The bifurcation diagrams (local maximum of the time series) with respect to J_{ie} in the interval [0, 5]. By changing the value of J_{ie}, the model is not capable of exhibiting chaos. **a** Excitatory membrane potential v_e, **b** inhibitory membrane potential v_i, and **c** adaptive parameter

5 Conclusion

Recently, a simple model has been proposed for describing the up and down state transitions in the neocortical neuronal networks composed of groups of excitatory and inhibitory neurons. The up and down state oscillations are relevant to some neuronal events such as slow wave sleep. Some studies have shown the existence of chaotic behavior during sleep. Motivated by this, in this paper, we investigate this model with the aim of finding chaotic behavior. The model consists of four synaptic strengths as excitatory–excitatory synaptic strength, excitatory–inhibitory synaptic strength, inhibitory–excitatory synaptic strength, and inhibitory–inhibitory synaptic strength. To present a complete analysis of the behavior of this model, we studied its dynamics with Lyapunov exponents and bifurcation diagrams in various synaptic strength values. The results showed that by altering the strength of the synaptic connection of the excitatory neurons to excitatory neurons, the chaotic behavior is observed in a wide range. The change in the synaptic strength of the excitatory neurons to the inhibitory neurons and also the inhibitory neurons to inhibitory neurons, led to an increment of the period of oscillations from period-1 to period-4. Also, varying the value of the inhibitory–excitatory neurons caused the changing of the oscillations period. Finally, the effect of the averaged adaptive parameter was investigated. It was obtained that

Table 6 The transitions between different dynamics of the model by J_{ie} variation in the range of [0, 5] (LE_1, LE_2, and LE_3 denote the three Lyapunov exponents)

Parameter range	Lyapunov exponents value	Dynamical behavior		
		v_e	v_i	c
$0 \leq J_{ie} < 0.585$	At $J_{ie} = 0.292$	Period 1	Period 1	Period 1
	$LE_1 = -92.77, LE_2 = -21.02, LE_3 \approx 0$			
$0.585 \leq J_{ie} < 0.62$	At $J_{ie} = 0.600$	Period 3	Period 3	Period 3
	$LE_1 = -87.69, LE_2 = -7.01, LE_3 \approx 0$			
$0.62 \leq J_{ie} < 0.675$	At $J_{ie} = 0.647$	Period 4	Period 4	Period 4
	$LE_1 = -86.19, LE_2 = -6.34, LE_3 \approx 0$			
$0.675 \leq J_{ie} < 0.71$	At $J_{ie} = 0.692$	Period 3	Period 3	Period 3
	$LE_1 = -85.31, LE_2 = -5.64, LE_3 \approx 0$			
$0.71 \leq J_{ie} < 1.1$	At $J_{ie} = 0.845$	Period 4	Period 4	Period 1
	$LE_1 = -82.18, LE_2 = -3.39, LE_3 \approx 0$			
$1.1 \leq J_{ie} < 5$	At $J_{ie} = 2.990$	Fixed point	Fixed point	Fixed point
	$LE_1 = -28.95, LE_2 = -28.55, LE_3 = -3.68$			

Table 7 The transitions between different dynamics of the model by Δc variation in the range of [0, 5] (LE_1, LE_2, and LE_3 denote the three Lyapunov exponents)

Parameter range	Lyapunov exponents value	Dynamical behavior		
		v_e	v_i	c
$0 \leq \Delta c < 0.026$	At $\Delta c = 0.013$	Period 1	Period 1	Period 1
	$LE_1 = -55.40, LE_2 = -1.20, LE_3 \approx 0$			
$0.026 \leq \Delta c < 5$	At $\Delta c = 2.630$	Fixed point	Fixed point	Fixed point
	$LE_1 = -99.20, LE_2 = -50.76, LE_3 = -1.92$			

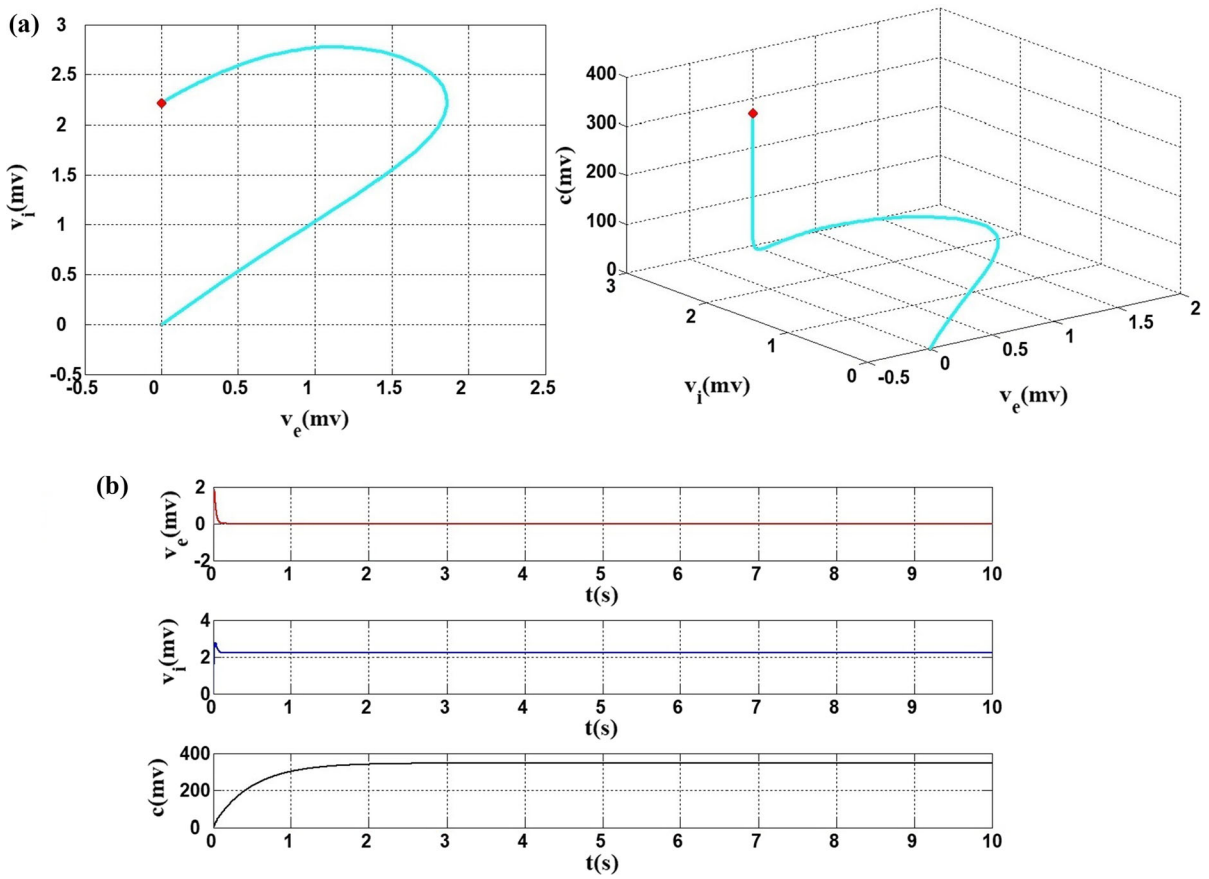

Fig. 12 The transition of the network to the fixed point at $\Delta c = 1$. **a** The cyan line indicates the system's transition from an initial condition to the fixed point in phase portrait. **b** The time series of three variables v_e, v_i, and c

this parameter should be very small for stimulating the neurons to fire. Otherwise, the level of adaptation $C(t)$ is high such that the excitatory neurons cannot stimulate other neurons, as a result of decreased neuronal activity.

Acknowledgements Matjaž Perc was supported by the Slovenian Research Agency (Grant Nos. J4-9302, J1-9112, and P1-0403).

Compliance with ethical standards

Conflict of interest The authors declare that they have no conflict of interest.

References

1. Ma, J., Tang, J.: A review for dynamics in neuron and neuronal network. Nonlinear Dyn. **89**(3), 1569–1578 (2017)
2. Hickok, G.: The Myth of Mirror Neurons: The Real Neuroscience of Communication and Cognition. WW Norton & Company, New York (2014)
3. Takagi, H.: Roles of ion channels in EPSP integration at neuronal dendrites. Neurosci. Res. **37**(3), 167–171 (2000)
4. Coombs, J., Eccles, J.C., Fatt, P.: The specific ionic conductances and the ionic movements across the motoneuronal membrane that produce the inhibitory post-synaptic potential. J. Physiol. **130**(2), 326–373 (1955)
5. Ma, J., Yang, Z.-Q., Yang, L.-J., Tang, J.: A physical view of computational neurodynamics. J. Zhejiang Univ A. Sci. **20**(9), 639–659 (2019)
6. Hashemi, N.S., Dehnavi, F., Moghimi, S., Ghorbani, M.: Slow spindles are associated with cortical high frequency activity. NeuroImage **189**, 71–84 (2019)
7. Ghorbani, M., Mehta, M., Bruinsma, R., Levine, A.J.: Nonlinear-dynamics theory of up-down transitions in neocortical neural networks. Phys. Rev. E **85**(2), 021908 (2012)
8. Song, X., Wang, C., Ma, J., Tang, J.: Transition of electric activity of neurons induced by chemical and electric autapses. Sci. China Technol. Sci. **58**(6), 1007–1014 (2015)
9. Koch, C., Segev, I., et al.: Methods in Neuronal Modeling: From Ions to Networks. MIT Press, Cambridge (1998)
10. Hodgkin, A.L., Huxley, A.F.: A quantitative description of membrane current and its application to conduction and excitation in nerve. J. Physiol. **117**(4), 500–544 (1952)
11. Nossenson, N., Messer, H.: Optimal sequential detection of stimuli from multiunit recordings taken in densely populated brain regions. Neural Comput. **24**(4), 895–938 (2012)
12. FitzHugh, R.: Impulses and physiological states in theoretical models of nerve membrane. Biophys. J. **1**(6), 445 (1961)
13. Nagumo, J., Arimoto, S., Yoshizawa, S.: An active pulse transmission line simulating nerve axon. Proc. IRE **50**(10), 2061–2070 (1962)
14. Hindmarsh, J.L., Rose, R.: A model of neuronal bursting using three coupled first order differential equations. Philos. Trans. R. Soc. Lond. Ser. B **221**(1222), 87–102 (1984)
15. Morris, C., Lecar, H.: Voltage oscillations in the barnacle giant muscle fiber. Biophys. J. **35**(1), 193–213 (1981)
16. Fourcaud-Trocmé, N., Hansel, D., Van Vreeswijk, C., Brunel, N.: How spike generation mechanisms determine the neuronal response to fluctuating inputs. J. Neurosci. **23**(37), 11628–11640 (2003)
17. Panahi, S., Rostami, Z., Rajagopal, K., Namazi, H., Jafari, S.: Complete dynamical analysis of myocardial cell exposed to magnetic flux. Chin. J. Phys. **64**, 363–373 (2020)
18. Parastesh, F., Rajagopal, K., Karthikeyan, A., Alsaedi, A., Hayat, T., Pham, V.-T.: Complex dynamics of a neuron model with discontinuous magnetic induction and exposed to external radiation. Cog. Neurodyn. **12**(6), 607–614 (2018)
19. Majhi, S., Ghosh, D.: Alternating chimeras in networks of ephaptically coupled bursting neurons. Chaos **28**(8), 083113 (2018)
20. Xu, Y., Jia, Y., Ma, J., Hayat, T., Alsaedi, A.: Collective responses in electrical activities of neurons under field coupling. Sci. Rep. **8**(1), 1–10 (2018)
21. Lv, M., Wang, C., Ren, G., Ma, J., Song, X.: Model of electrical activity in a neuron under magnetic flow effect. Nonlinear Dyn. **85**(3), 1479–1490 (2016)
22. Lv, M., Ma, J.: Multiple modes of electrical activities in a new neuron model under electromagnetic radiation. Neurocomputing **205**, 375–381 (2016)
23. Wu, F., Ma, J., Zhang, G.: A new neuron model under electromagnetic field. Appl. Math. Comput. **347**, 590–599 (2019)
24. Xu, Y., Ma, J., Zhan, X., Jia, Y.: Temperature effect on memristive ion channels. Cognit. Neurodyn. **13**(6), 601–611 (2019)
25. Parastesh, F., Azarnoush, H., Jafari, S., Hatef, B., Perc, M., Repnik, R.: Synchronizability of two neurons with switching in the coupling. Appl. Math. Comput. **350**, 217–223 (2019)
26. Majhi, S., Bera, B.K., Ghosh, D., Perc, M.: Chimera states in neuronal networks: a review. Phys. Life Rev. **28**, 100–121 (2019)
27. Sun, X., Perc, M., Kurths, J.: Effects of partial time delays on phase synchronization in Watts–Strogatz small-world neuronal networks. Chaos **27**(5), 053113 (2017)
28. Majhi, S., Perc, M., Ghosh, D.: Chimera states in a multilayer network of coupled and uncoupled neurons. Chaos **27**(7), 073109 (2017)
29. Kundu, S., Majhi, S., Ghosh, D.: Chemical synaptic multiplexing enhances rhythmicity in neuronal networks. Nonlinear Dyn. **98**(3), 1659–1668 (2019)
30. Vaidyanathan, S.: Adaptive control of the Fitzhugh–Nagumo chaotic neuron model. Int. J. Pharm. Technol. Res. **8**(6), 117–127 (2015)
31. Lakshmanan, S., Lim, C.P., Nahavandi, S., Prakash, M., Balasubramaniam, P.: Dynamical analysis of the Hindmarsh–Rose neuron with time delays. IEEE Trans. Neural Netw. Learn. Syst. **28**(8), 1953–1958 (2016)
32. Panahi, S., Jafari, S., Khalaf, A.J.M., Rajagopal, K., Pham, V.-T., Alsaadi, F.E.: Complete dynamical analysis of a neuron under magnetic flow effect. Chin. J. Phys. **56**(5), 2254–2264 (2018)
33. Middleton, J., Chacron, M., Lindner, B., Longtin, A.: Firing statistics of a neuron model driven by long-range correlated noise. Phys. Rev. E **68**(2), 021920 (2003)
34. Channell, P., Fuwape, I., Neiman, A.B., Shilnikov, A.L.: Variability of bursting patterns in a neuron model in the presence of noise. J. Comput. Neurosci. **27**(3), 527 (2009)
35. Kang, Q., Huang, B., Zhou, M.: Dynamic behavior of artificial Hodgkin–Huxley neuron model subject to additive noise. IEEE Trans. Cybern. **46**(9), 2083–2093 (2015)
36. Wilson, C.J., Kawaguchi, Y.: The origins of two-state spontaneous membrane potential fluctuations of neostriatal spiny neurons. J. Neurosci. **16**(7), 2397–2410 (1996)
37. Marshall, L., Helgadóttir, H., Mölle, M., Born, J.: Boosting slow oscillations during sleep potentiates memory. Nature **444**(7119), 610–613 (2006)
38. Wolansky, T., Clement, E.A., Peters, S.R., Palczak, M.A., Dickson, C.T.: Hippocampal slow oscillation: a novel eeg state and its coordination with ongoing neocortical activity. J. Neurosci. **26**(23), 6213–6229 (2006)
39. Mehta, M.R.: Cortico–Hippocampal interaction during up-down states and memory consolidation. Nat. Neurosci. **10**(1), 13–15 (2007)

40. Stickgold, R.: Sleep-dependent memory consolidation. Nature **437**(7063), 1272–1278 (2005)
41. Sanchez-Vives, M.V., Mattia, M., Compte, A., Perez-Zabalza, M., Winograd, M., Descalzo, V.F., Reig, R.: Inhibitory modulation of cortical up states. J. Neurophysiol. **104**(3), 1314–1324 (2010)
42. Tokdar, S., Xi, P., Kelly, R.C., Kass, R.E.: Detection of bursts in extracellular spike trains using hidden semi-Markov point process models. J. Comput. Neurosci. **29**(1–2), 203–212 (2010)
43. Ji, D., Wilson, M.A.: Coordinated memory replay in the visual cortex and hippocampus during sleep. Nat. Neurosci. **10**(1), 100–107 (2007)
44. Babloyantz, A., Salazar, J., Nicolis, C.: Evidence of chaotic dynamics of brain activity during the sleep cycle. Phys. Lett. A **111**(3), 152–156 (1985)
45. Hirata, Y., Oku, M., Aihara, K.: Chaos in neurons and its application: perspective of chaos engineering. Chaos Interdiscip. J. Nonlinear Sci. **22**(4), 047511 (2012)
46. Rasmussen, R., Jensen, M.H., Heltberg, M.L.: Chaotic dynamics mediate brain state transitions, driven by changes in extracellular ion concentrations. Cell Syst. **5**(6), 591–603 (2017)
47. Shi, W., Shang, P., Ma, Y., Sun, S., Yeh, C.-H.: A comparison study on stages of sleep: quantifying multiscale complexity using higher moments on coarse-graining. Commun. Nonlinear Sci. Numer. Simul. **44**, 292–303 (2017)
48. Dahal, P., Avagyan, M., Skardal, P.S., Blaise, H.J., Ning, T.: Characterizing chaotic behavior of REM sleep EEG using lyapunov exponent. In: 2017 10th International Congress on Image and Signal Processing, BioMedical Engineering and Informatics, pp. 1–6. IEEE (2017)
49. Diekelmann, S., Born, J.: The memory function of sleep. Nat. Rev. Neurosci. **11**(2), 114–126 (2010)
50. Rasch, B., Born, J.: About sleep's role in memory. Physiol. Rev. **93**(2), 681–766 (2013)
51. Fuhrmann, G., Markram, H., Tsodyks, M.: Spike frequency adaptation and neocortical rhythms. J. Neurophys. **88**(2), 761–770 (2002)
52. Boeing, G.: Visual analysis of nonlinear dynamical systems: chaos, fractals, self-similarity and the limits of prediction. Systems **4**(4), 37 (2016)
53. Guckenheimer, J., Holmes, P.: Nonlinear Oscillations, Dynamical Systems, and Bifurcations of Vector Fields, vol. 42. Springer, Berlin (2013)